ELSEVIER

Contents lists available at ScienceDirect

Journal of Human Evolution

journal homepage: www.elsevier.com/locate/jhevol



Examination of magnitudes of integration in the catarrhine vertebral column



Hyunwoo Jung*, Evan A. Simons, Noreen von Cramon-Taubadel

Buffalo Human Evolutionary Morphology Lab, Department of Anthropology, University at Buffalo, SUNY, Buffalo, NY, USA

ARTICLE INFO

Article history: Received 12 January 2021 Accepted 27 March 2021 Available online 18 May 2021

Keywords: Morphological integration Integration coefficient of variation Vertebrae Morphological evolution

ABSTRACT

The evolution of novel vertebral morphologies observed in humans and other extant hominoids may be related to changes in the magnitudes and/or patterns of covariation among traits. To examine this, we tested magnitudes of integration in the vertebral column of cercopithecoids and hominoids, including humans. Three-dimensional surface scans of 14 vertebral elements from 30 Cercopithecus, 32 Chlorocebus, 39 Macaca, 45 Hylobates, 31 Pan, and 86 Homo specimens were used. A resampling method was used to generate distributions of integration coefficient of variation scores for vertebral elements individually using interlandmark distances. Interspecific comparisons of mean integration coefficient of variation were conducted using Mann-Whitney U tests with Bonferroni adjustment. The results showed that hominoids generally had lower mean integration coefficient of variation than cercopithecoids. In addition, humans showed lower mean integration coefficient of variation than other hominoids in their last thoracic and lumbar vertebrae. Cercopithecoids and Hylobates showed relatively lower mean integration coefficient of variation in cervical vertebrae than in thoracolumbar vertebrae. Pan and Homo showed relatively lower mean integration coefficient of variation in the last thoracic and lumbar vertebrae in the thoracolumbar region, except for the L1 of Pan. The results suggest fewer integrationmediated constraints on the evolution of vertebral morphology in hominoids when compared with cercopithecoids. The weaker magnitudes of integration in lumbar vertebrae in humans when compared with chimpanzees likewise suggest fewer constraints on the evolution of novel lumbar vertebrae morphology in humans.

© 2021 Elsevier Ltd. All rights reserved.

1. Introduction

Morphological integration has been of interest to morphologists for decades, especially as integration among traits may result in a correlated response to selection in those traits (Olson and Miller, 1958; Cheverud, 1982; Marroig and Cheverud, 2005; Porto et al., 2009; Marroig et al., 2009; de Oliveira et al., 2009; Young et al., 2010; Williams, 2010; Rolian et al., 2010; Grabowski et al., 2011; Conaway et al., 2018; Villamil, 2018; Arlegi et al., 2018, 2020). Thus, the theoretical framework of morphological integration, which seeks to understand and explain patterns of covariation among traits, can be informative for interpreting routes of morphological evolution. For example, the framework of morphological integration has been used in studies of modern humans to understand how complex and novel morphological traits may have evolved

through long-term interactions among those traits (Cheverud, 1996; Hallgrímsson et al., 2009). For instance, strong morphological integration among modules may need to first be dissociated or differently structured for novel morphological evolution to occur (Cheverud, 1982; Hallgrímsson et al., 2009; Young et al., 2010; Armbruster et al., 2014; Goswami et al., 2014; Klingenberg, 2014). Because of this, it is critical to consider morphological integration when interpreting evolutionary processes of traits as selection on one trait can result in correlated responses in other traits that are not themselves under selection. Alternatively, responses to selection on one trait may be constrained because of correlation or covariation with other traits that are under stabilizing selection (Cheverud, 1996; Hansen and Houle, 2008; Hallgrímsson et al., 2009). In addition, trait variation that results from an initial correlated response or as an evolutionary by-product may become advantageous later (i.e., an exaptation; Gould and Lewontin, 1979; Gould and Vrba, 1982). For instance, it has been suggested that the morphological evolution of hominin fingers may be a correlated

E-mail address: hjung26@buffalo.edu (H. Jung).

^{*} Corresponding author.

response to developmental constraints and the by-product of stronger selection pressures on toes in association with bipedal locomotion (Rolian et al., 2010). From this, it can be inferred that morphological covariation between homologous elements, such as hands and feet, may play a large role in possible routes of morphological evolution. Morphological integration is, therefore, an important theoretical framework as it demonstrates that many traits cannot necessarily be considered as independent units with straightforward adaptive explanations (Olson and Miller, 1958; Hallgrímsson et al., 2009; Armbruster et al., 2014; Goswami et al., 2014; Klingenberg, 2014).

The theoretical framework of morphological integration has also been used to investigate how integration among skeletal elements may facilitate and/or constrain morphological diversification in primates (Cheverud, 1982; Ackermann and Cheverud, 2000, 2002; Marroig and Cheverud, 2004; Lawler, 2008; Porto et al., 2009; Marroig et al., 2009; Goswami and Polly, 2010; Young et al., 2010; Williams, 2010; Rolian et al., 2010; Grabowski et al., 2011; Villmoare et al., 2011; Lewton, 2012; Savell et al., 2016; Conaway et al., 2018; Villamil, 2018; Arlegi et al., 2018, 2020; Jung et al., 2021). For example, Cheverud and colleagues used a quantitative genetics approach to examine morphological integration and its evolutionary consequences in the cranial morphology of mammals, including primates (Cheverud, 1982; Marroig and Cheverud, 2005; Porto et al., 2009; Marroig et al., 2009; de Oliveira et al., 2009; Shirai and Marroig, 2010). These studies often differentiate between patterns of integration, which refers to the way traits are correlated, and magnitudes of integration, which compares the relative strength of that correlation (Porto et al., 2009). Thus, it is possible for magnitudes to differ while patterns are similar or vice versa (Porto et al., 2009; Marroig et al., 2009). For instance, patterns of integration in the mammalian cranium have been found to be relatively constant while the magnitudes of integration vary (Porto et al., 2009; Marroig et al., 2009).

Previous investigations have found that hominoids, and especially humans, have relatively weaker magnitudes of integration in the cranium than other anthropoids, which was taken to indicate fewer constraints on the evolution of cranial morphology (Porto et al., 2009; de Oliveira et al., 2009). In addition, in studies of morphological integration in the primate postcranial skeleton, hominoids showed weaker magnitudes of integration in homologous fore- and hindlimb modules, suggesting fewer constraints on the morphological evolution of novel limb proportions in hominoids compared with other anthropoids (Young et al., 2010). Thus, it can be inferred that the evolution of novel skeletal morphologies in the cranium (e.g., globularity) and limb bones (e.g., short arms and long legs) of humans might have been possible because of generally reduced magnitudes of integration and fewer constraints on morphological changes in hominoids.

However, few studies have examined morphological integration in the primate postcranial axial skeleton, even though vertebrae are well suited to examine the evolutionary consequences of morphological integration (Villamil, 2018; Arlegi et al., 2018, 2020). The vertebral column consists of homologous elements because of shared developmental pathways, such as somite differentiation and segregation from paraxial mesoderm, which are primarily regulated by the HOX gene family (Burke et al., 1995; Nowicki and Burke, 2000; Wellik, 2007). HOX gene expression domains have also been found to overlap in limb bones and the vertebral column (Wellik and Capecchi, 2003; Young et al., 2010). Because of this, in relation to HOX gene expression domains, human and other hominoids vertebrae may show reduced constraints in paths of morphological evolution, as is seen in limb bone proportions (Young et al., 2010). For instance, HOX9 and HOX10 regulate development in both the fore- and hindlimb as well as in the thoracic and lumbar vertebrae

(Wellik and Capecchi, 2003; Young et al., 2010). Thus, it is possible that the factors that led to the reduced magnitudes of integration observed in hominoid limb bone proportions may also be present in the vertebral column. However, the few studies that have been conducted on primate vertebrae have only examined the neck region, including the cranial base (or chondrocranium) and/or cervical vertebrae in orthograde hominoids (Arlegi et al., 2018: Villamil, 2018). Morphological integration in the entire vertebral column has been investigated in humans (Arlegi et al., 2020), where it was found that lower thoracic and lumbar vertebrae show weaker magnitudes of integration (and were therefore likely to be more evolvable) than cervical and upper thoracic vertebrae, which may be associated with the evolution of bipedal locomotion and related morphological changes in lumbar vertebrae (e.g., vertebral body wedging and lumbar lordosis). However, it has not yet been examined whether this intervertebral variation in magnitudes of integration can also be found in other hominoids. Thus, without comparing them to other primate taxa, it may be premature to conclude that humans are particularly unique when it comes to intervertebral variation in magnitudes of integration. Moreover, it is currently unknown whether magnitudes of integration are different across the axial skeleton of catarrhines. A comparative approach is therefore critical for examining characteristics of morphological integration in the primate axial skeleton to better understand how integration may have affected morphological evolution in the cranial and postcranial skeletal elements of humans.

In this regard, two related predictions will be tested in this study:

Prediction 1: Hominoids have less integrated vertebrae compared with cercopithecoids. Previous studies have found weaker magnitudes of integration in hominoids than in cercopithecoids for both cranial (Porto et al., 2009) and limb data (Young et al., 2010). In a similar vein, it is expected that magnitudes of integration in vertebrae also will be weaker in hominoids than cercopithecoids.

Prediction 2: Humans have less integrated vertebrae compared with other hominoids. Previous studies have reported that modern humans showed weaker magnitudes of integration than other hominoids in both the cranium (Porto et al., 2009) and the pelvis (Grabowski et al., 2011). Thus, it was inferred that weaker magnitudes of integration were related to fewer constraints on the evolution of cranial and pelvic morphology in the human lineage (Porto et al., 2009; Grabowski et al., 2011). Thus, we predict that magnitudes of integration in vertebrae will be weaker in humans than in other hominoids. Alternatively, humans may show similar magnitudes of integration to other hominoids, as has been observed in their limb bones (Young et al., 2010).

2. Materials and methods

2.1. Sample

In this study, 15 Cercopithecus ascanius, 15 Cercopithecus mitis, 20 Chlorocebus aethiops, 12 Chlorocebus pygerythrus, 39 Macaca fascicularis, 45 Hylobates lar, 31 Pan troglodytes, and 86 Homo sapiens were used (Table 1). Two species each in Cercopithecus and Chlorocebus were combined in this study to reach a minimum sample size of 30 individuals. Only adult specimens were used. Adult status was assessed based on the third molar being in full occlusion and/or a (fully) fused spheno-occipital synchondrosis. Individuals with any missing vertebra or not identifiable landmarks in the midline or in both left and right sides were excluded from this study. These specimens are housed in the Cleveland Museum of Natural History, the Smithsonian Museum of Natural History, the Field Museum of

Table 1Sample description and controlled variation.

Taxa	Sex			Controlled variation
	Male	Female	Total	
Cercopithecus ascanius	9	6	15	S, SP, T, L
Cercopithecus mitis	8	7	15	
Chlorocebus aethiops	11	9	20	S, SP, WC, T, L
Chlorocebus pygerythrus	6	6	12	
Macaca fascicularis	22	17	39	S, WC, T, L
Hylobates lar	22	23	45	S, L, SAC
Pan troglodytes	16	15	31	S, T, L, SAC
Homo sapiens	48	38	86	S

Abbreviations: S = sex; SP = species; WC = wild vs. captive; T = identity of the last thoracic vertebra; <math>L = identity of the last lumbar vertebra; <math>SAC = the number of sacral vertebrae.

Natural History, the Museum of Comparative Zoology at the Harvard University, the Forensic Anthropology Center at the University of Tennessee-Knoxville, the Neil C. Tappen Collection at the University of Minnesota, the American Museum of Natural History, and the Department of Anthropology of the University at Buffalo, SUNY. Thirty specimens were set as the minimum sample size to calculate the magnitude of integration using the integration coefficient of variation (ICV), as demonstrated by Jung et al. (2020). In morphological integration studies, one issue that has been consistently debated is how many specimens are required for the reliable calculation of patterns and magnitudes of integration (e.g., Cheverud, 1988; Ackermann, 2009; Adams, 2016; Grabowski and Porto, 2017; Jung et al., 2020). Cheverud and colleagues (e.g., Cheverud, 1988; Ackermann, 2009) suggested that 40 specimens may be a sufficient sample size for estimating the structure of the variance/covariance matrix, whereas Adams (2016) reported that the covariance ratio coefficient is not sensitive to sample size for calculating degrees of modularity. In contrast, Grabowski and Porto (2017) suggested that at least 108 specimens are required for calculating magnitudes of integration in humans with trait correlations having an average R² of 0.05. More in line with Cheverud and colleagues (e.g., Cheverud, 1988; Ackermann, 2009), Jung et al. (2020) reported that magnitudes of integration can be reliably calculated with at least 30 specimens using mean ICV calculated using a resampling method when the average trait R² is reasonably high (e.g., $R^2 > 0.08$), which was the case in this study (Supplementary Online Material [SOM] Table S1). Thus, the sample size was not considered to be a hindering factor here as magnitudes of integration (mean ICV) were calculated based on a trait resampling method with at least 30 specimens per taxon.

2.2. Data collection methods

Five cervical (C1, C2, C3, C5, and C7), five thoracic (T1, T4, T7, T10, and T12/13), three lumbar vertebrae, and the sacrum were examined to assess differences in magnitudes of integration. In total, 3682 vertebral elements from 263 individuals were scanned and analyzed in this study. About half of the vertebral column was selected in this study as vertebral elements share developmental origins (i.e., somite differentiation and segregation from paraxial mesoderm) and genetic controls (i.e., HOX gene family; Burke et al., 1995; Nowicki and Burke, 2000; Wellik, 2007). Moreover, adjacent vertebrae share functional roles within vertebral regions and show similar morphologies after C3 (Shapiro, 1993; Been et al., 2019). Thus, it can be assumed that selected parts of the vertebral column in this study can be a proxy for the general trend of magnitudes of integration in the vertebral column as a whole. Five cervical, five thoracic, and three lumbar vertebrae were sampled for each individual. For the cervical vertebrae, C1 and C2 were included given their distinct morphology. C3 was selected as C3 is the first cervical vertebra after C2 and has a distinctive morphology relative to C2. C5 and C7 were included as C7 is the last cervical vertebra and C5 is located midway between C3 and C7. For the thoracic vertebrae, the first and last thoracic vertebrae were sampled, as well as the vertebrae halfway along the thoracic spine (T7) and two vertebrae approximately equidistant between the ends and the midpoint (T4 and T10). Thoracic vertebrae are defined as rib-bearing vertebrae within the thoracolumbar vertebral column (Williams et al., 2016). Thus, the last in the rib-bearing vertebrae was used as the last thoracic vertebra, which in some species is T12, whereas in others is T13. For lumbar vertebrae, three elements were chosen as there are some individuals with only three lumbar vertebrae (e.g., Pan and Gorilla). In Cercopithecus, Chlorocebus, and Macaca, L1, L4, and L6/7 were used as there are either six or seven lumbar vertebrae (Williams, 2012). In Pan and Gorilla, L1, L2, and L3/4 were used as there are either three or four lumbar vertebrae (Williams, 2012). In Hylobates, L1, L3, and L5/6 were used as there are either five or six lumbar vertebrae (Williams, 2012). In Homo, L1, L3, and L5 were used as there are five lumbar vertebrae (Williams, 2012). In Homo, all individuals we sampled had 12 thoracic, five lumbar, and five sacral vertebrae. In case of the possibly fused coccygeal vertebra to the sacrum, it was regarded as the first coccygeal vertebra when the cornua of that coccygeal vertebra projects superiorly to meet the sacral cornua that project inferiorly (Russo and Williams, 2015). In addition, the apex and base of the sacral hiatus was examined by their location to assess the status of coccygeal vertebra. Russo and Williams (2015) showed that, in humans, the apex and base of the hiatus is located at the penultimate sacral vertebra and at the ultimate sacral vertebra in most cases, respectively, although the location of hiatus may be highly variable in other hominoids (Machnicki et al., 2016).

Three-dimensional surface scans of vertebral elements were produced with an HDI-120 and a Macro R5X structured-light scanner (LMI technologies Inc., Vancouver, Canada). To maximize sample size, landmarks were digitized on the left side using the software Landmark (Wiley et al., 2005; Table 2; Fig. 1) by a single researcher (HJ). In a few cases, the right side of the vertebra was used when the left side was damaged. In the case of bifurcated (or bituberculosity) spinous processes in cervical vertebrae, the average coordinates between the left and right sides of the bituberculosity in the spinous process were used. The last rib-bearing vertebra with a costal facet on only one side was treated as the last thoracic vertebra. The left side was landmarked as in other vertebral elements unless there was marked bilateral asymmetry for the location of landmarks on the vertebral body. In the case of marked asymmetry, the side with the costal facet was landmarked. For partially sacralized last lumbar vertebra, the left side was landmarked as in other vertebral elements unless there was marked bilateral asymmetry for the location of landmarks on the transverse process and/or vertebral body. In the case of marked asymmetry, the side without sacralization was landmarked. Partially sacralized last lumbar vertebrae were found in only two humans and one chimpanzee, and the impacted side was only slightly or moderately sacralized and the last lumbar vertebra could be disarticulated from the sacrum. Variation attributable to sex, species, wild vs. captive, identity of the last thoracic or lumbar vertebrae, and/or the number of sacral vertebrae was controlled by mean centering within each genus (Table 1). Mean centering is "the act of subtracting a variable's mean from all observations on the variable in the data set such that the variable's new mean is zero" (Iacobucci et al., 2016: 1308). For instance, in the case of C1 of Cercopithecus, mean centering was conducted by each sex to control the difference in means between the distributions of males and females. Thus, mean centering of variable X in males was conducted

 Table 2

 Description of the landmarks used in this study.

Landmarks	Anatomical description	Measurement error (mm)
C1		
1	The most ventral point of the base of the ventral tubercle in the midline	0.086
2	The most dorsal and middle point of the dorsal arch in the midline	0.108
3	The most craniodorsal point of the dorsal arch in the midline	0.035
4	The most caudodorsal point of the dorsal arch in the midline	0.025
5	The most cranioventral point of the vertebral foramen in the midline	0.031
6	The most lateral point on the transverse process	0.054
7	The most medial point on the cranial articular facet	0.113
8	The most lateral point on the cranial articular facet	0.076
9	The most ventral point on the cranial articular facet	0.033
10	The most dorsal point in the cranial articular facet	0.088
11	The most lateral point on the caudal intervertebral articular facet	0.083
12	The most medial point on the caudal intervertebral articular facet	0.189
13	The most ventral point on the caudal intervertebral articular facet	0.085
14	The most dorsal point on the caudal intervertebral articular facet	0.045
C2		
1	The most dorsal point of the spinous process in the midline	0.028
2	The most caudoventral point of the vertebral body in the midline	0.039
3	The most caudodorsal point of the vertebral body in the midline	0.051
1	The most caudolateral point of the vertebral body	0.053
5	The most craniodorsal of the vertebral foramen in the midline	0.027
5	The most ventral point of the superior articular facet	0.052
7	The most dorsal point of the superior articular facet	0.018
3	The most medial point of the superior articular facet	0.103
)	The most lateral point of the superior articular facet	0.054
0	The most cranial point on the dens in the midline	0.081
11	The most (cranio)lateral point on the dens	0.101
12	The most dorsal point of the base of dens in the midline	0.081
13	The most ventral point of the base of dens in the midline	0.055
14	The most lateral point on the transverse process	0.061
15	The most (caudo)lateral point on the caudal intervertebral articular facet	0.051
C3 — Lumbar vertebrae		
1	The most (cranio)dorsal point of the spinous process in the midline	0.129
2	The most cranioventral point of the vertebral body in the midline	0.061
3	The most craniodorsal point of the vertebral body in the midline	0.029
1	The most craniolateral point of the vertebral body ³ (or the uncinate process in the cervical vertebrae)	0.065
· •	The most caudoventral point of the vertebral body in the midline	0.099
5	The most caudodorsal point of the vertebral body in the midline	0.076
7	The most caudolateral point of the vertebral body ^a	0.141
3	The most craniodorsal point of the vertebral foramen in the midline	0.047
)	The most lateral point on the transverse process	0.101
0	The most (dorso)lateral point on the caudal intervertebral articular facet	0.119
1	The most (dorso)lateral point on the cranial intervertebral articular facet	0.049
12	The most medial point on the cranial intervertebral articular facet	0.056
Sacrum	The most median point on the cramar mervercesian articular facet	0.030
l	The most ventral point of the vertebral articular surface in the midline	0.042
2	The most dorsal point of the vertebral articular surface in the midline	0.174
3	The most lateral point of the vertebral articular surface	0.139
4	The most caudoventral point of the caudal articular surface	0.119
5	The most lateral point of the caudal articular surface	0.115
5 5	The most raderal point of the caudal articular surface The most medial point of the most cranioventral sacral foramen	0.115
7	The most craniolateral point of the most cranioventral sacrar foramen	0.113
, 8	The most cramolateral point of the auricular surface	0.105
o 9	The most (dorso)lateral point of the adricular surface The most (dorso)lateral point on the vertebral articular facet	0.103
9 10	The most medial point on the vertebral articular facet	0.067
10	the most mediai point on the vertebrai articular facet	0.007

^a Excluding costal facet in the thoracic vertebrae.

by subtracting the mean of variable X in males from the value of variable X in each male specimen. The same procedure was conducted for female specimens. Next, mean centering was conducted by each species using the result of mean centering by each sex. To assess intraobserver error, the C1, C2, T7, and sacrum of one *M. fascicularis* were digitized three times, and error was calculated in millimeters (mm) for each landmark (Table 2). Error assessment is based on standard deviations among coordinates of landmarks on three-dimensional models because each scan shares the same fixed coordinated plane (von Cramon-Taubadel et al., 2007). Mean measurement error was 0.045 mm in C1, 0.056 mm in C2, 0.081 mm in T7, and 0.107 mm in the sacrum.

2.3. Analytical methods

Magnitudes of integration based on the ICV were calculated by first computing all possible Euclidean distances between landmarks, and then using these distances to calculate the variation among eigenvalues of covariance matrices based on the Euclidean distances. There were 91 variables in C1, 105 variables in C2, 66 variables in C3 through the last lumbar vertebra, and 45 variables in the sacrum. High ICV indicate that most of the shape variation is concentrated within fewer dimensions, as ICV = $\frac{\sigma(\lambda)}{\overline{\lambda}}$, where $\sigma(\lambda)$ is the standard deviation of the eigenvalues and $\overline{\lambda}$ is the mean of those

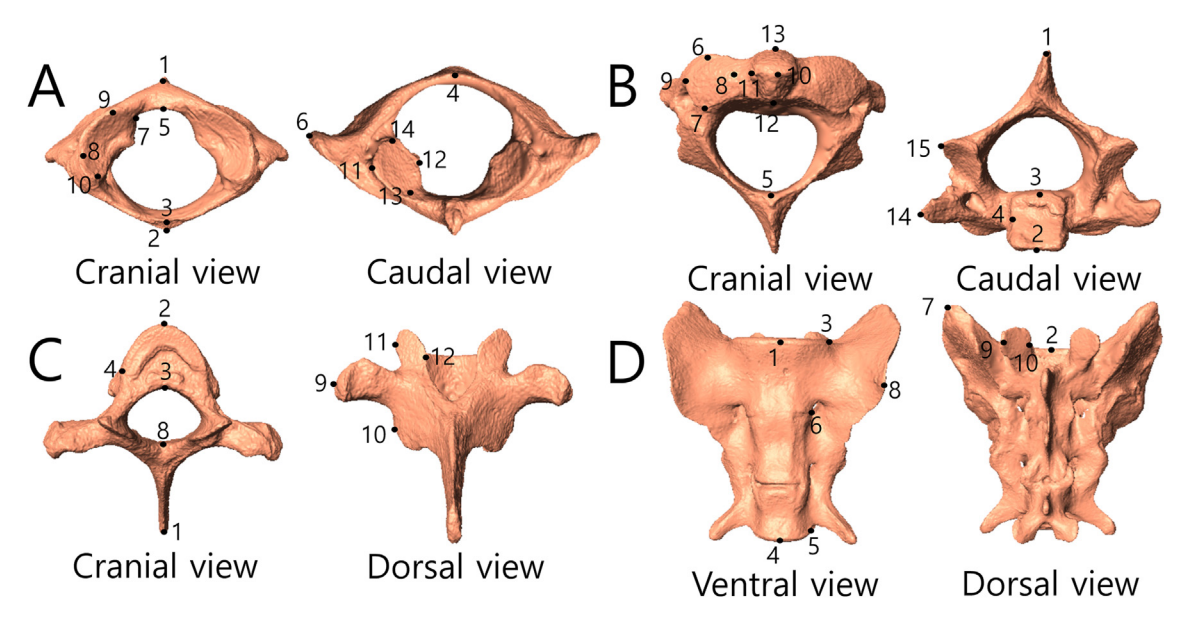


Figure 1. Landmarks on the left side of vertebrae and sacrum of Macaca fascicularis. A: C1; B: C2; C: T7; D: sacrum.

eigenvalues (Shirai and Marroig, 2010; Jung et al., 2020). Moreover, ICV is scale independent, as the standard deviation of eigenvalues is standardized by its mean. ICV was calculated using variance—covariance (V/CV) matrices based on each vertebral element separately. A resampling method was applied to generate distributions of ICV values for each vertebral element based on interlandmark distances (Conaway et al., 2018; Jung et al., 2020). This resampling method uses 10 traits (i.e., the interlandmark distances), which are randomly resampled 1000 times from the total number of available traits. Thus, the mean and standard deviation of ICV values were generated based on 1000 random sets of vectors. Then, these distributions of ICV values were statistically compared across vertebral elements.

Comparisons of mean ICV among catarrhine taxa were conducted using Mann-Whitney U tests with Bonferroni adjustment (i.e., statistically significant when p < 0.003 for 15 Mann–Whitney U tests within each vertebra and the sacrum). After comparisons among taxa, rank scores were assigned to each taxon based on whether they had significantly stronger or weaker magnitudes of integration compared with other taxa. Rank scores were not calculated when the comparison result was not statistically significant. Thus, a higher rank score means relatively stronger magnitudes of integration than other taxa. For example, C1 in Homo showed mean ICV that were significantly lower than three taxa, significantly higher than one taxon, and not significantly different from one taxon (SOM Table S2). Thus, rank scores of C1 in Homo were -2. Rank scores were devised to succinctly show how magnitudes of integration in each vertebral element significantly differ from other taxa as there were six catarrhine taxa and fourteen vertebral elements in this study. By using rank scores, the results of Mann-Whitney U tests could be presented in a single figure or table (e.g., Table 4 and Fig. 3). The detailed results of Mann–Whitney U tests for interspecific comparisons are presented in SOM Tables S2-S15. Next, comparisons of mean ICV among vertebral elements were conducted within each taxon using Mann-Whitney U tests with Bonferroni adjustment (i.e., statistically significant when p < 0.00055 for 91 Mann–Whitney U tests within each species). The same rank scoring method described earlier was also applied to each vertebral element. The detailed results of Mann-Whitney U tests for intervertebral comparisons within each taxon are presented in SOM Tables S16-S21.

Calculation of ICV was conducted using the 'CalcICV' function in the evolgg package (Melo et al., 2015) in R v. 3.6.3 (R Core Team, 2020). Mann—Whitney U tests were also conducted using R v. 3.6.3.

3. Results

3.1. Interspecific comparison

The results showed that hominoids generally have lower mean ICV than cercopithecoids (Figs. 2 and 3; Tables 3 and 4; SOM Tables S2—S15), and therefore weaker magnitudes of integration in the vertebral column. However, there were some exceptions. In *Pan*, C3 and the sacrum had relatively higher mean ICV than other taxa. In *Homo*, C2 and the sacrum had relatively higher mean ICV than most taxa.

Among cercopithecoids, *Chlorocebus* and *Macaca* showed relatively higher mean ICV in C1, C5, C7, and in the thoracolumbar vertebrae than *Cercopithecus*, except for the last lumbar vertebra. *Macaca* also showed relatively higher mean ICV in C2, C3, C5, the thoracic vertebrae, and the sacrum than other cercopithecoids (Fig. 2; Table 3).

Among hominoids, *Hylobates* showed relatively lower mean ICV than *Pan* and *Homo* in cervical vertebrae and the sacrum, but relatively higher mean ICV in T4, T7, and the middle and last lumbar vertebrae (Fig. 2; Table 3). *Pan* showed relatively lower mean ICV in T4, but relatively higher mean ICV in C3, C5, L1, and the sacrum than other hominoids. Humans showed relatively lower mean ICV in their last thoracic and lumbar vertebrae but relatively higher mean ICV in C2, C7, and T1 than other hominoids.

3.2. Intervertebral variation of mean integration coefficient of variation within each species

In general, cercopithecoids showed lower mean ICV in cervical vertebrae than the thoracolumbar vertebrae (Figs. 2 and 4; Table 5; SOM Tables S16—S21). *Hylobates* showed a similar intervertebral variation of mean ICV to cercopithecoids but with lower mean ICV. *Pan* and *Homo* showed relatively lower mean ICV in the last thoracic and lumbar vertebrae (Fig. 2; Table 5). Moreover, *Pan* and *Homo* showed relatively higher mean ICV in their central thoracic vertebrae within the thoracolumbar region. There was also a difference

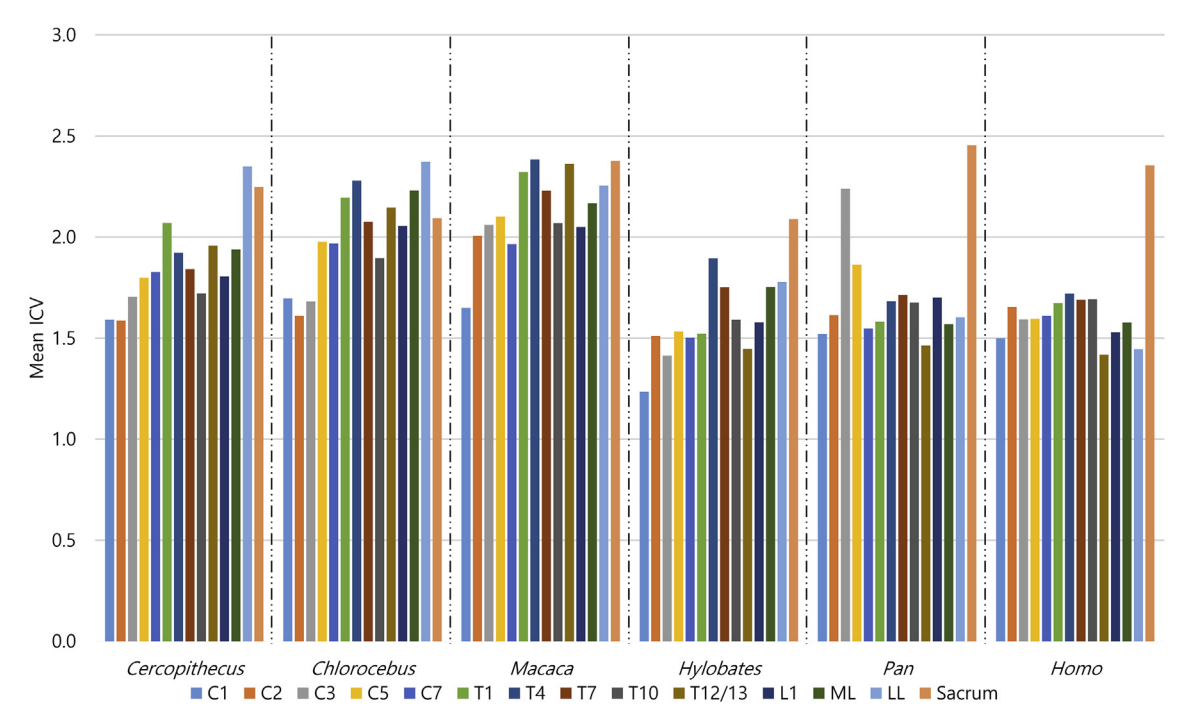


Figure 2. Mean integration coefficient of variation in the catarrhine vertebral column. ICV = integration coefficient of variation; ML = middle lumbar vertebra; LL = last lumbar vertebra.

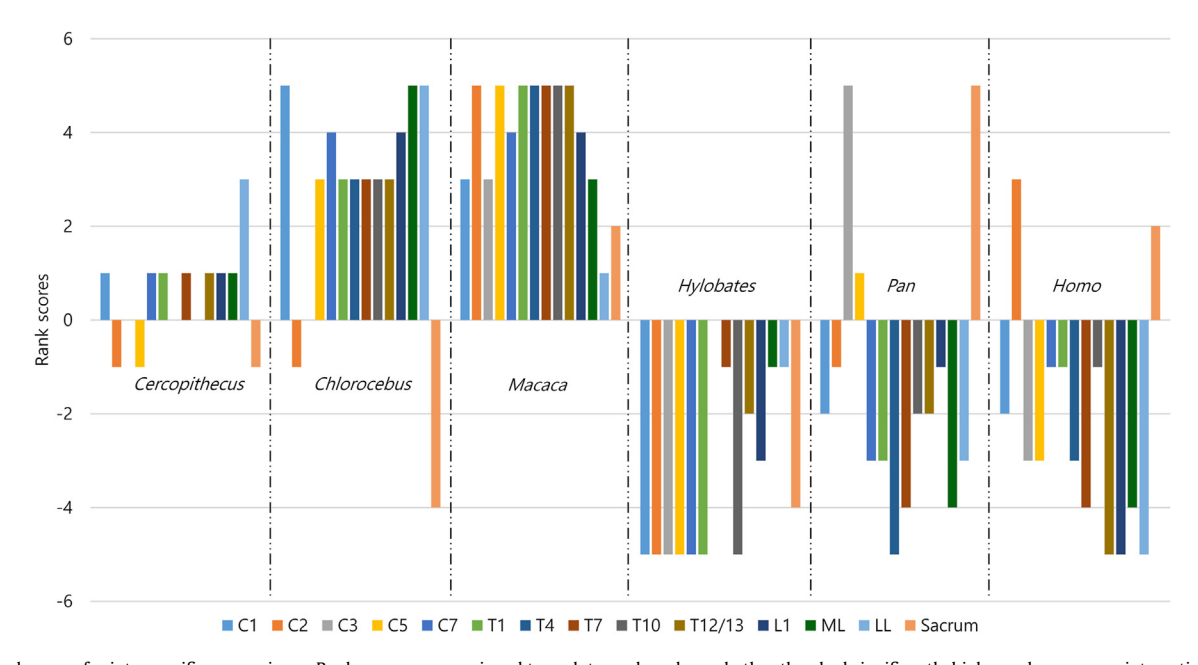


Figure 3. Rank scores for interspecific comparisons. Rank scores were assigned to each taxon based on whether they had significantly higher or lower mean integration coefficient of variation compared with other taxa using Mann—Whitney U tests. Rank scores were not calculated when the comparison result was not statistically significant. Thus, a higher rank score means relatively stronger magnitudes of integration than other taxa. ML = middle lumbar vertebra; LL = last lumbar vertebra.

between *Pan* and *Homo* as *Pan* showed much higher mean ICV in C3 and C5 than *Homo*. All three hominoid taxa showed relatively higher mean ICV in the sacrum than in other vertebrae (Fig. 2). A common feature in all six catarrhine taxa in this study was that the atlas (C1) showed the lowest or the second lowest mean ICV among cervical vertebrae (C1 and C2 mean ICV were not significantly different in *Cercopithecus*, C1 and C3 mean ICV were not significantly different in *Chlorocebus*, and C1 and C7 mean ICV were not significantly different in *Pan*; Fig. 2; Table 3; SOM Tables S16—S21).

Some boundary vertebrae between vertebral regions (e.g., T1) showed generally higher mean ICV than other vertebrae for cercopithecoids in the thoracolumbar region (Figs. 2 and 4; Tables 3 and 5). In *Cercopithecus* and *Chlorocebus*, T1 and the last lumbar vertebrae showed relatively higher mean ICV, whereas the last thoracic vertebra showed intermediate mean ICV. In *Macaca*, T1 and T12/13 showed relatively higher mean ICV, whereas C7, L1, and the last lumbar vertebra showed intermediate mean ICV. In cercopithecoids, C1 showed relatively lower mean ICV. Moreover, T4

Table 3Mean integration coefficient of variation (with standard deviation in parenthesis) in vertebral elements.

Vertebral elements	Taxa					
	Cercopithecus	Chlorocebus	Масаса	Hylobates	Pan	Ното
C1	1.592 (0.25)	1.697 (0.16)	1.650 (0.17)	1.235 (0.14)	1.520 (0.18)	1.499 (0.15)
C2	1.586 (0.20)	1.611 (0.18)	2.006 (0.18)	1.511 (0.21)	1.613 (0.20)	1.654 (0.19)
C3	1.705 (0.15)	1.681 (0.19)	2.060 (0.17)	1.413 (0.22)	2.240 (0.42)	1.593 (0.19)
C5	1.799 (0.19)	1.976 (0.19)	2.101 (0.17)	1.533 (0.23)	1.863 (0.33)	1.595 (0.20)
C7	1.827 (0.24)	1.968 (0.23)	1.965 (0.19)	1.502 (0.27)	1.547 (0.23)	1.611 (0.23)
T1	2.070 (0.19)	2.194 (0.25)	2.322 (0.22)	1.522 (0.23)	1.582 (0.21)	1.673 (0.19)
T4	1.922 (0.19)	2.279 (0.29)	2.384 (0.24)	1.895 (0.22)	1.682 (0.20)	1.720 (0.17)
T7	1.841 (0.20)	2.076 (0.25)	2.230 (0.22)	1.752 (0.19)	1.714 (0.21)	1.689 (0.19)
T10	1.721 (0.18)	1.896 (0.17)	2.069 (0.20)	1.592 (0.21)	1.676 (0.19)	1.692 (0.21)
T12/13	1.957 (0.18)	2.146 (0.18)	2.363 (0.17)	1.447 (0.17)	1.463 (0.19)	1.418 (0.19)
L1	1.805 (0.20)	2.055 (0.20)	2.050 (0.20)	1.578 (0.22)	1.700 (0.20)	1.528 (0.20)
ML	1.938 (0.21)	2.231 (0.24)	2.167 (0.18)	1.753 (0.21)	1.569 (0.18)	1.577 (0.19)
LL	2.349 (0.15)	2.373 (0.15)	2.255 (0.14)	1.778 (0.19)	1.603 (0.18)	1.445 (0.19)
Sacrum	2.248 (0.24)	2.093 (0.18)	2.376 (0.19)	2.089 (0.26)	2.454 (0.26)	2.355 (0.24)

Abbreviations: ML = middle lumbar vertebra; LL = last lumbar vertebra.

Table 4Rank scores for interspecific comparisons.

Vertebral elements	Taxa					
	Cercopithecus	Chlorocebus	Масаса	Hylobates	Pan	Ното
C1	1	5	3	-5	-2	-2
C2	-1	-1	5	-5	-1	3
C3	0	0	3	-5	5	-3
C5	-1	3	5	-5	1	-3
C7	1	4	4	-5	-3	-1
T1	1	3	5	-5	-3	-1
T4	0	3	5	0	-5	-3
T7	1	3	5	-1	-4	-4
T10	0	3	5	-5	-2	-1
T12/13	1	3	5	-2	-2	-5
L1	1	4	4	-3	-1	-5
ML	1	5	3	-1	-4	-4
LL	3	5	1	-1	-3	-5
Sacrum	-1	-4	2	-4	5	2

Abbreviations: ML = middle lumbar vertebra; LL = last lumbar vertebra.

Rank scores were assigned to each taxon based on whether they had significantly higher or lower mean ICV compared with other taxa using Mann—Whitney U tests. Rank scores were not calculated when the comparison result was not statistically significant. Thus, a higher rank score means relatively stronger magnitudes of integration than other taxa

showed relatively higher mean ICV than T1 and T12/13 in *Chlorocebus* and *Macaca*. In contrast, hominoids showed generally lower mean ICV in the boundary vertebrae. In *Hylobates*, C1 and T12/13 showed relatively lower mean ICV, whereas C7, T1, L1, and the last lumbar vertebra showed intermediate mean ICV. In *Pan*, C1, C7, and T12/13 showed relatively lower mean ICV, whereas T1, L1, and the last lumbar vertebra showed intermediate mean ICV. In *Homo*, C1, T12, and the last lumbar vertebra showed relatively lower mean ICV, whereas C7 and T1 showed intermediate mean ICV. In hominoids, T4 also showed higher mean ICV than T1 and T12/13 like in *Chlorocebus* and *Macaca*.

4. Discussion

4.1. Comparison between hominoids and cercopithecoids

The interspecific comparisons demonstrated that hominoids have weaker magnitudes of integration than cercopithecoids (Table 3; Fig. 2). This result corresponds to previous studies on the cranium (Porto et al., 2009) and limb bones (Young et al., 2010). Thus, the first prediction — the hominoids have less integrated vertebrae compared with cercopithecoids — was supported by these results, indicating that there may be fewer constraints on

morphological evolution in hominoid vertebrae than in cercopithecoids.

Comparisons of patterns of vertebral integration within taxa showed variation in intervertebral magnitudes of integration between cercopithecoids and hominoids. The vertebral column consists of homologous elements due to shared developmental pathways, which are primarily regulated by the HOX gene family (Burke et al., 1995). HOX gene expression domains are generally distinct between vertebral regions (i.e., the cervical, thoracic, lumbar, and sacral regions), which can be conceived of as developmental modules. Nevertheless, there are overlaps of HOX gene expression between vertebral regions, such as the thoracolumbar region, likely resulting in correlated responses to selection between vertebral regions due to the overlapping effects and domains of HOX gene expression (Wellik, 2007). Thus, increased morphological variation may be expected in boundary vertebrae (Shapiro and Kemp, 2019). The results of this study showed that cercopithecoids generally had stronger magnitudes of integration in T1, T12/ 13, and/or the last lumbar vertebra, whereas hominoids generally had weaker magnitudes of integration in C1, T12/13, and/or the last lumbar vertebra (Figs. 2 and 4). Nevertheless, cercopithecoids also showed relatively weak magnitudes of integration in C1 and/or C7. Moreover, T4 was more integrated than T1 and T12/13 in all taxa except Cercopithecus. Thus, this study found only partial support

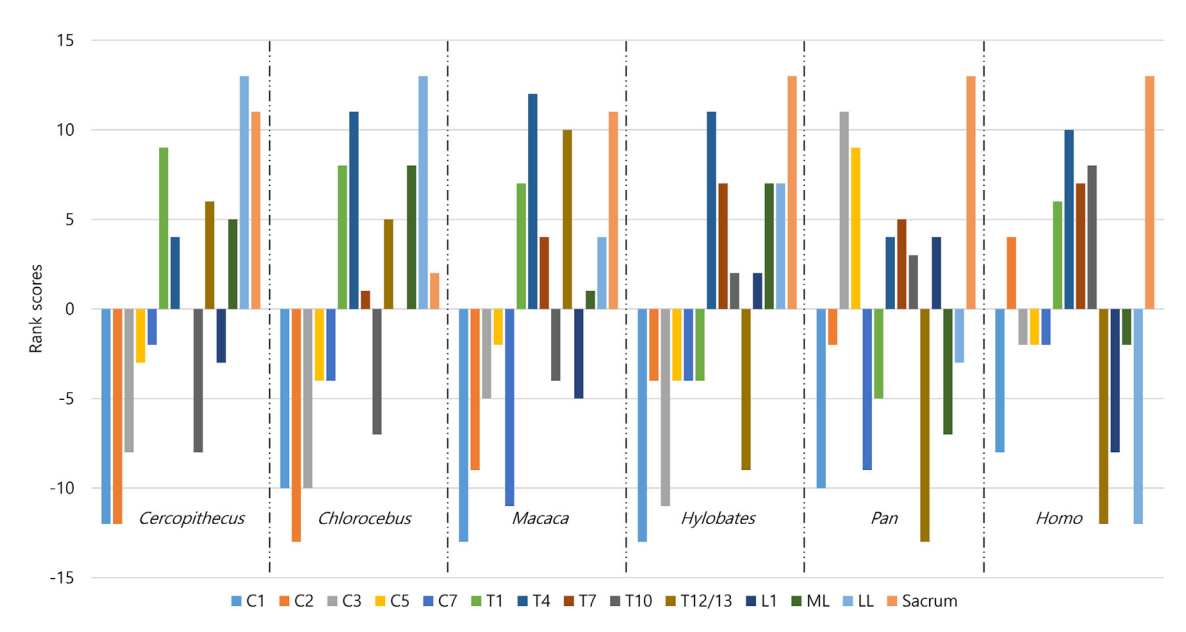


Figure 4. Rank scores for intervertebral comparisons within each taxon. Rank scores were assigned to each vertebral element based on whether they had significantly higher or lower mean integration coefficient of variation compared with other vertebral elements using Mann—Whitney U tests. Rank scores were not calculated when the comparison result was not statistically significant. Thus, a higher rank score means relatively stronger magnitudes of integration than other vertebral elements within each taxon. ML = middle lumbar vertebra: I.I. = last lumbar vertebra.

Table 5Rank scores for intervertebral comparisons within each taxon

Vertebral elements	Taxa						
	Cercopithecus	Chlorocebus	Масаса	Hylobates	Pan	Ното	
C1	-12	-10	-13	-13	-10	-8	
C2	-12	-13	-9	-4	-2	4	
C3	-8	-10	-5	-11	11	-2	
C5	-3	-4	-2	-4	9	-2	
C7	-2	-4	-11	-4	-9	-2	
T1	9	8	7	-4	-5	6	
T4	4	11	12	11	4	10	
T7	0	1	4	7	5	7	
T10	-8	-7	-4	2	3	8	
T12/13	6	5	10	-9	-13	-12	
L1	-3	0	-5	2	4	-8	
ML	5	8	1	7	-7	-2	
LL	13	13	4	7	-3	-12	
Sacrum	11	2	11	13	13	13	

Abbreviations: ML = middle lumbar vertebra; LL = last lumbar vertebra.

Rank scores were assigned to each vertebral element based on whether they had significantly higher or lower mean ICV compared with other vertebral elements using Mann—Whitney U tests. Rank scores were not calculated when the comparison result was not statistically significant. Thus, a higher rank score means relatively stronger magnitudes of integration than other vertebral elements within each taxon.

from cercopithecoids that boundary vertebrae have relatively stronger magnitudes of integration. This result should be interpreted with caution as the magnitudes of integration in the last thoracic and/or the last lumbar vertebra may be affected by the 'intermediate status' of boundary vertebra, such as the costal facet being on only one side of the last thoracic vertebra or because of partially sacralized last lumbar vertebra. Nevertheless, in general, hominoids showed relatively weaker magnitudes of integration than cercopithecoids in most vertebral elements, and not just in the last thoracic or the last lumbar vertebra.

Overall intervertebral variation in magnitudes of integration was generally similar between cercopithecoids and *Hylobates*, and between *Pan* and *Homo* (Table 5; Figs. 2 and 4). Cercopithecoids and *Hylobates* showed relatively stronger magnitudes of integration in thoracolumbar vertebrae than cervical vertebrae, although *Hylobates* had weaker magnitudes of integration overall than

cercopithecoids. The similarities between cercopithecoids and Hylobates suggest that the catarrhine last common ancestor (LCA) might have had similar intervertebral variation in magnitudes of integration as those observed in these taxa, though further testing with a larger taxonomic representation is necessary. Similar intervertebral variations in magnitudes of integration have also been reported in felids (Randau and Goswami, 2017). Randau and Goswami (2017) showed that magnitudes of integration in vertebrae increased caudally starting from T10, with the last lumbar vertebra having the largest magnitudes. From this, Randau and Goswami (2017) suggested that stronger morphological integration in T10-L7 of felids may not only constrain the direction of morphological variation but also facilitate the amount of morphological variation along that vector in morphospace in relation to locomotory specialization. Strong morphological integration may facilitate the amount of response to selection when the selection

vector and the 'Pmax' (i.e., the first principal component axis) have a similar direction in morphospace (Marroig et al., 2009). In the present study, cercopithecoids and Hylobates showed relatively stronger magnitudes of integration in thoracolumbar vertebrae than cervical vertebrae (Table 5; Figs. 2 and 4). Thoracolumbar vertebrae of primates also show morphological variation in relation to locomotor behaviors (Shapiro, 1993; Johnson and Shapiro, 1998). For instance, cercopithecoids have longer lumbar vertebrae (e.g., relatively higher craniocaudal length of the vertebral body) for extension and flexion movement during leaping and/or running (Shapiro, 1993). However, hylobatids have different locomotor patterns, such as ricochetal brachiation and suspensory behavior (Fleagle, 2013), which is absent in cercopithecoids. Thus, it is possible that the similar intervertebral variation in magnitudes of integration seen in cercopithecoids and Hylobates may be a primitive mammalian feature, and thus shared with felids, but not particular association with locomotor specialization. But again, further phylogenetic comparative analyses need to be conducted before this can be confirmed.

Although Hylobates and Pan/Homo varied in their intervertebral variation in magnitudes of integration, they all showed generally weaker magnitudes of integration than cercopithecoids (Tables 3 and 4; Figs. 2 and 3). Hylobates showed generally stronger magnitudes of integration in the thoracolumbar vertebrae than in the cervical vertebrae, similar to what was observed in cercopithecoids. Nevertheless, there was a clear trend toward hominoids having weaker magnitudes of integration than cercopithecoids (Tables 3 and 4; Figs. 2 and 3). Weaker magnitudes of integration in hominoid limb bones (Young et al., 2010) and vertebrae may be related to a similar developmental mechanism, namely the HOX gene family. For instance, weaker magnitudes of integration in caudally located vertebrae may be related to the mutations in HOX9 and HOX10 that also regulate fore- and hindlimb development (Wellik and Capecchi, 2003; Young et al., 2010). For instance, HOX9 quadruple mutants affect the eighth thoracic through the fourth lumbar vertebrae, and HOX10 triple mutants affect the first lumbar through the fourth sacral element in experimental mutant mice studies (Wellik, 2007). Thus, dissociation between homologous fore- and hindlimbs (Young et al., 2010) and within lower thoracic and lumbar vertebrae may be related to similar developmental mechanisms. These reduced magnitudes of integration in limb bone and vertebral elements during the evolutionary history of hominoids may have resulted in fewer constraints, which in turn may have led to a proliferation of morphologies and locomotor behaviors. In Miocene apes, various locomotor repertoires, from generalized arboreal quadrupeds to more below-branch arboreal activities (e.g., suspensory), have been suggested based on limb bone and vertebral morphology (reviewed in Alba, 2012; Ward, 2015; Pilbeam and Lieberman, 2017). The Early and Middle Miocene apes Morotopithecus and Pierolapithecus were suggested to have had below branch forelimb dominated locomotor behavior (Sanders and Bodenbender, 1994; Nakatsukasa, 2008, 2019). Their vertebral morphology is similar to hylobatids in having short bodies, and in the location of their transverse processes (e.g., as in Morotopithecus, where they arise from the junction between the vertebral body and the pedicle; Sanders and Bodenbender, 1994; Nakatsukasa, 2008, 2019). Also, it was suggested that the torso of some Miocene apes showed a broadening and stiffness similar to that of extant apes, but to a smaller degree (Alba, 2012; Ward, 2015; Pilbeam and Lieberman, 2017). The Late Miocene apes Oreopithecus, Hispanopithecus, and Rudapithecus are suggested to have locomotor behaviors more similar to extant apes than to earlier Miocene forms (Russo and Shapiro, 2013; Susanna et al., 2014; Ward, 2015; Pilbeam and Lieberman, 2017; but see Ward et al., 2019 for an argument based on os coxa morphology that Rudapithecus had an orthograde body posture and a below-branch arboreal locomotor repertoire with a somewhat longer and more flexible lumbar spine than extant great apes). For example, Hispanopithecus shows transverse processes from a short and robust pedicle, which is similar to extant great apes (Susanna et al., 2014). In contrast, the Early and Middle Miocene apes Proconsul, Nacholapithecus, Eauatorius, and Griphopithecus were more akin to generalized arboreal quadrupeds (Ward, 1993, 2015; Kikuchi et al., 2015; Pilbeam and Lieberman, 2017). In addition, their torso was narrow, and their lower back was long as seen in extant cercopithecoids (Ward, 1993, 2015; Kikuchi et al., 2015; Pilbeam and Lieberman, 2017). Recently, the small-bodied and gibbon-like late Middle Miocene (11.6 Ma) ape Pliobates was suggested to have mixed traits for generalized arboreal quadrupeds (e.g., primitive proximal humeral morphology) and suspensory behaviors (e.g., the reduced ulnocarpal articulation; Alba et al., 2015). Moreover, the late Middle Miocene (11.62 Ma) ape Danuvius is claimed to have extended limb clambering and even hominin-like bipedalism for locomotor behavior based on postcranial morphology (e.g., almost perpendicular orientation of tibial angle relative to the horizontal plane of the ankle joint; Böhme et al., 2019), although its locomotory repertoire is still debated (Williams et al., 2020). Thus, a mosaic of derived and primitive postcranial morphologies existed during the evolutionary radiation and proliferation of Miocene apes (Begun, 2010; Alba, 2012; Begun et al., 2012; Ward, 2015), and although it has not been measured in these extinct apes, it is a distinct possibility that magnitudes of integration in the vertebral column would be weaker, similar to what is observed in extant hominoids. In sum, the various combinations of derived and primitive vertebral morphologies in Miocene apes may have been related to weaker magnitudes of integration and the resultant reduction of constraints on paths of diversification. The developmental mechanisms discussed earlier (i.e., the HOX gene family) may have had a role in lowering magnitudes of integration and in restructuring torso and limb bone morphology in Miocene apes.

The stronger magnitudes of integration in the hominoid sacrum relative to other vertebrae are possibly connected to the loss of the hominoid tail. Cercopithecoids showed either similar or weaker magnitudes of integration between the sacrum and other vertebrae (Fig. 2; Table 3), indicating that the cercopithecoid sacrum may need relatively weaker magnitudes of integration to respond to morphological variation in both pre/post-sacral vertebrae and tail use. For instance, the sacrum's caudal articular surface significantly varies between tail length categories (i.e., tail-less, (very) short, and long-tailed catarrhines; Russo and Shapiro, 2011). More circularity in the caudal articular surface of the sacrum may provide more mobility in the tail (Russo and Shapiro, 2011). Moreover, the sacrocaudal articulation angle is more acute in long-tailed cercopithecoids than (very)short-tailed ones, which may enhance tail extension during leaping (Russo and Shapiro, 2011). Thus, tail uses that are reflected in overall sacral morphology may also be related to the similar magnitudes of integration in the sacrum (than other vertebrae) within cercopithecoids. There is also more intraspecific variation in the number of sacral vertebrae in hominoids than cercopithecoids (Williams, 2012), which may result in different magnitudes of integration in the sacrum of these taxa. In this study, there was variation in the number of sacral vertebrae in Hylobates and Pan, which was controlled by a mean centering procedure. However, the humans we sampled only had five sacral vertebrae, and the magnitudes of integration in the human sacrum were still stronger than other vertebral elements and similar to the chimpanzee sacrum. Considering these results, higher intraspecific variability in the number of sacral vertebrae may not be a critical factor for calculating magnitudes of integration in the hominoid sacrum. More hominoid taxa (e.g., gorillas and orangutans) need to be analyzed to examine whether the magnitudes of integration in the sacrum of hominoids are influenced by the higher intraspecific variability in the number of sacral vertebrae.

Although the main focus of this section was to compare magnitudes of integration between cercopithecoids and hominoids, we also noticed a common feature in intervertebral variation in magnitudes of integration in this study. In the six catarrhine taxa examined here, the atlas (C1) was the least or the second least integrated vertebra among cervical vertebrae (Fig. 2; Table 3; SOM Tables S16-S21). Relatively weaker magnitudes of integration in the atlas may be related to the interaction between the cranium and the atlas. It has been suggested that atlas morphology may be related to several factors. For instance, Manfreda et al. (2006) reported that orthograde species show thinner anterior and posterior arches, a more ventrally and caudally oriented transverse process, and a more inclined and laterally rounded superior articular facets than pronograde species. Nalley and Grider-Potter (2017) showed that skull size and neck posture (e.g., neck inclination angle) were associated with some atlas shape variation, such as the width or craniocaudal length of posterior arches, respectively. In contrast, Linden et al. (2019) argued that shape variation in the atlas was largely explained by body size and phylogenetic relatedness (but not by locomotor behaviors and head size) among the orders Primates, Rodentia, Lagomorpha, Dermoptera, and Scandentia, Thus, there is little consensus regarding the possible factors that may explain morphological variation in the atlas. Moreover, variation in atlas morphology may be driven in part by craniofacial morphology, as Villamil (2018) found high levels of integration (relative variance of eigenvalues) between the atlas and the basicranium among cervical vertebrae, and because the basicranium is the 'central integrator' of overall craniofacial morphology (Lieberman, 2011). Further studies that directly investigate the relationship between morphological integration in the atlas and locomotor behaviors, skull shape and size, neck posture, and/or phylogenetic relations are needed to explain the relatively weaker magnitudes of integration in the atlas found in this study.

In addition, some differences among cercopithecoids are worth mentioning (Figs. 2 and 3; Tables 3 and 4). Among cercopithecoids, Chlorocebus and Macaca showed relatively stronger magnitudes of integration in C1, C5, C7, and the thoracolumbar vertebrae than Cercopithecus, except for the last lumbar vertebra. Macaca also showed relatively stronger magnitudes of integration in C2, C3, C5, the thoracic vertebrae, and in the sacrum than other cercopithecoids. Thus, in general, Cercopithecus showed relatively weaker magnitudes of integration, whereas Macaca showed relatively stronger magnitudes of integration among cercopithecoids. Therefore, it should be noted that there is variation in the magnitudes of integration among cercopithecoids, and thus that the constraints on morphological evolution may also vary within cercopithecoids, even though they all have generally stronger magnitudes of integration in the vertebral column when compared with hominoids. For instance, Cercopithecus may have lower levels of constraints on the morphological evolution of the vertebral column than Chlorocebus and Macaca. Nevertheless, it is hard to infer why Cercopithecus showed relatively weaker magnitudes of integration at this point. Further studies with more cercopithecoid groups (e.g., colobines and papionins) and other primate taxa as outgroup (e.g., platyrrhines) are needed to show what features (e.g., degrees of arboreality) are related to generally weaker magnitudes of integration in the vertebral column of Cercopithecus when compared with Chlorocebus and Macaca.

4.2. Comparison between humans and other hominoids

The second prediction tested here was also partially supported, as humans generally showed weaker magnitudes of integration in their last thoracic and lumbar vertebrae compared to other hominoids (Table 3: Fig. 2). Thus, humans have undergone a further reduction in magnitudes of integration in the last thoracic and lumbar vertebrae relative to other hominoids, as has also been observed in the cranium (Porto et al., 2009) and pelvis (Grabowski et al., 2011). There are several morphological changes in human lumbar vertebrae associated with bipedal locomotion. For instance, humans have the largest consecutive increases in surface area of the lumbar vertebral body among hominoids (Latimer and Ward, 1993; Shapiro, 1993). In humans, there are larger consecutive decreases in the lengths of postzygapophyseal joints of lumbar vertebrae when compared to chimpanzees, which is related to the lordotic curve (i.e., lumbar lordosis; Latimer and Ward, 1993). In relation to lumbar lordosis, humans also show high degrees of dorsal wedging in the lumbar vertebral body, which is absent in chimpanzees (Latimer and Ward, 1993). Lumbar lordosis due to vertebral wedging means a higher craniocaudal height of the ventral side of the vertebral body than the dorsal side (Latimer and Ward, 1993). The relatively larger surface area of lumbar vertebral bodies and lumbar lordosis is related to upright bipedal locomotion in humans, such as moving the center of mass of the torso over the sacroiliac and the hip joints (Latimer and Ward, 1993; Shapiro, 1993). Young et al. (2010) have suggested that the evolution of novel limb bone proportions in humans (i.e., short arms and long legs) related to obligate bipedal locomotion was facilitated by fewer constraints, which itself was the product of a dissociation of limb bone covariation that was likely already present in hominoid clade. In a similar vein, the evolution of novel vertebral morphology in humans may have been less constrained by weaker magnitudes of integration in vertebrae. Reduced levels of covariation may have facilitated morphological changes in the lumbar region through an increased flexibility for responding to novel selective pressures in relation to obligate bipedalism. Thus, further dissociation of covariation in lumbar vertebral morphology may have occurred in humans before or with the evolution of obligate bipedalism.

The intervertebral variation in magnitudes of integration in humans found in the present investigation corresponds to a previous study (Arlegi et al., 2020), which showed that humans have weaker magnitudes of integration in more caudally located vertebrae (e.g., lumbar region). Moreover, both Arlegi et al. (2020) and the present study showed that central thoracic vertebrae in humans showed relatively stronger magnitudes of integration compared to other vertebrae. The results of the present study demonstrated that intervertebral variation in magnitudes of integration is not unique to humans, as it is also shared with chimpanzees in the thoracolumbar region. Thus, the LCA of Pan and Homo might also have similar intervertebral variation in magnitudes of integration as found here for Pan and Homo. However, it is also possible that intervertebral variation in magnitudes of integration in Pan and Homo changed independently in each lineage. Despite the similarity, intervertebral variation in magnitudes of integration between Pan and Homo was generally different in the cervical vertebrae (Tables 3 and 5; Figs. 2 and 4). Chimpanzees showed much stronger magnitudes of integration in C3 and C5, but weaker magnitudes of integration in C2 and C7 when compared with humans (Table 3; Fig. 2). Similar results were also reported in Arlegi et al. (2018), where chimpanzees and gorillas had higher levels of integration in C3 than humans. Villamil (2018) also reported that chimpanzees had relatively higher levels of integration (relative variance in eigenvalues) in C5 compared with humans. This may be related to the biomechanical characteristics of the more prognathic face and well-developed neck muscles of chimpanzees when compared with humans (Lieberman, 2011). For instance, the spinous process in C3 and C5 of chimpanzees is elongated compared with humans, which provides longer leverage to the neck muscles for balancing the skull (Nalley and Grider-Potter, 2015). Thus, C3 and C5 in chimpanzees may have stronger magnitudes of integration related to functional demands (Villamil. 2018; Arlegi et al., 2018, 2020). Thus, intervertebral variation in magnitudes of integration may be shared between humans and chimpanzees in the thoracolumbar vertebrae but not in cervical vertebrae because of similar developmental mechanisms (i.e., HOX gene family) and functional demands (i.e., balancing skull), respectively. In contrast to the present study, Arlegi et al. (2018) and Villamil (2018) reported that chimpanzees had relatively stronger integration in C7 than humans. It was argued in Arlegi et al. (2018) that relatively weaker integration in the human C7 may be associated with the appearance of the modern human-like morphology of C7 in KNM-WT 15000 (Homo erectus). Weaker morphological integration may result in a greater ability to respond to selection vectors, such as a more mobile neck during walking and running (Lieberman, 2011; Arlegi et al., 2018). In contrast, based on the results of the present study, humans may have relatively stronger magnitudes of integration in C7 relative to chimpanzees for increased stability during walking and running. Further investigations are needed to reconcile the discrepancy between this and previous studies.

Hylobates showed relatively weaker magnitudes of integration than Pan and Homo in the cervical vertebrae and sacrum, but relatively stronger magnitudes of integration in T4. T7. and the middle and last lumbar vertebrae (Fig. 2; Table 3). Villamil (2018) also reported that Hylobates had relatively weaker integration in C2, C3, C4, C5, and C7 than Pan and Homo. As mentioned earlier, intervertebral variation in magnitudes of integration in Hylobates may be a primitive mammalian feature, as it is shared with cercopithecoids and felids (Randau and Goswami, 2017). Alternatively, Hylobates may have distinct intervertebral magnitudes of integration that are derived relative to the ancestral hominoid state as Hylobates have a smaller body size and a more arboreal locomotor repertoire among hominoids (Fleagle, 2013). However, Grabowski and Jungers (2017) argued that the LCA of hominoids may be gibbon-sized (e.g., Pliobates), which is different from previous suggestions that hylobatids are a dwarf lineage from great apesized LCA of hominoids (Pilbeam, 1996). Thus, it is not certain only from the data in this study whether the intervertebral variation of magnitudes of integration in Hylobates reflects primitive mammalian features or further derivation from common hominoid features. Further studies are needed with more hominoids (e.g., gorillas and orangutans) and outgroup taxa to examine whether intervertebral variation in magnitudes of integration in Hylobates, Pan, or Homo is a general or unique feature among the apes.

5. Conclusion

In this study, magnitudes of integration were compared in the vertebral column between six catarrhine taxa: *Cercopithecus*, *Chlorocebus*, *Macaca*, *Hylobates*, *Pan*, and *Homo*. The results showed that hominoids generally had weaker magnitudes of integration in the vertebrae than cercopithecoids. Humans generally had weaker magnitudes of integration in the last thoracic and lumbar vertebrae than other hominoids. These results suggest that there might have been a dissociation in the levels of covariation within each vertebrae in hominoids, with a further reduction in human lumbar vertebrae. The similarity of intervertebral variation between humans and chimpanzees was mostly found in caudally located vertebrae (e.g., lumbar region). Humans showed weaker magnitudes of integration

in the lumbar region than chimpanzees. These results suggest that changes in intervertebral variation in magnitudes of integration may be related to the evolution of novel vertebral morphology, and may have played a role in the evolution of obligate bipedalism in humans. In future studies, more great apes (e.g., gorillas and orangutans) are needed to determine if the results observed in chimpanzees and humans are general features for great apes.

Author contributions

Hyunwoo Jung — conceptualization, data curation, formal analysis, investigation, visualization, and writing the original draft. Evan A. Simons — conceptualization, investigation, and supervision. Noreen von Cramon-Taubadel — conceptualization, investigation, supervision, and funding acquisition. All authors contributed critically to the drafts and gave final approval for publication.

Declaration of competing interest

None.

Acknowledgments

We thank the Editor, Associate Editor, an editorial board member, and three anonymous reviewers for their helpful and constructive comments on an earlier version of this manuscript. We are grateful to Yohannes Haile-Selassie at the Cleveland Museum of Natural History, Darrin Lunde at the Smithsonian Museum of Natural History, Lawrence Heaney at the Field Museum of Natural History, Mark Omura at the Museum of Comparative Zoology at the Harvard University, Dawnie Wolfe Steadman at the Forensic Anthropology Center at the University of Tennessee-Knoxville, and staffs at the Neil C. Tappen Collection at the University of Minnesota and the American Museum of Natural History for granting access to skeletal materials for data collection. We thank the SUNY Research Foundation for funding to support this research. This material is based upon work supported by the National Science Foundation under grant number BCS-1830745 and The Mark Diamond Research Fund of the Graduate Student Association at the University at Buffalo, the State University of New York.

Appendix A. Supplementary Online Material

Supplementary online material to this article can be found online at https://doi.org/10.1016/j.jhevol.2021.102998.

References

Ackermann, R.R., 2009. Morphological integration and the interpretation of fossil hominin diversity. Evol. Biol. 36, 149–156.

Ackermann, R.R., Cheverud, J.M., 2000. Phenotypic covariance structure in tamarins (genus *Saguinus*): a comparison of variation patterns using matrix correlation and common principal component analysis. Am. J. Phys. Anthropol. 111, 489–501.

Ackermann, R.R., Cheverud, J.M., 2002. Discerning evolutionary processes in patterns of tamarin (genus *Saguinus*) craniofacial variation. Am. J. Phys. Anthropol. 117. 260–271.

Adams, D.C., 2016. Evaluating modularity in morphometric data: challenges with the RV coefficient and a new test measure. Method. Ecol. Evol. 7, 565–572.

Alba, D.M., 2012. Fossil apes from the Vallès-Penedès basin. Evol. Anthropol. 21, 254–269

Alba, D.M., Almécija, S., DeMiguel, D., Fortuny, J., de los Ríos, M.P., Pina, M., Robles, J.M., Moyà-Solà, S., 2015. Miocene small-bodied ape from Eurasia sheds light on hominoid evolution. Science 350, aab2625.

Arlegi, M., Gómez-Robles, A., Gómez-Olivencia, A., 2018. Morphological integration in the gorilla, chimpanzee, and human neck. Am. J. Phys. Anthropol. 166, 408–416.

- Arlegi, M., Veschambre-Couture, C., Gómez-Olivencia, A., 2020. Evolutionary selection and morphological integration in the vertebral column of modern humans. Am. J. Phys. Anthropol. 171, 17–36.
- Armbruster, W.S., Pélabon, C., Bolstad, G.H., Hansen, T.F., 2014. Integrated phenotypes: understanding trait covariation in plants and animals. Phil. Trans. R Soc. B 369, 20130245.
- Been, E., Gómez-Olivencia, A., Kramer, P.A. (Eds.), 2019. Spinal Evolution: Morphology, Function, and Pathology of the Spine in Hominoid Evolution. Springer, Cham, Switzerland.
- Begun, D.R., 2010. Miocene hominids and the origins of the African apes and humans, Annu. Rev. Anthropol. 39, 67-84.
- Begun, D.R., Nargolwalla, M.C., Kordos, L., 2012. European Miocene hominids and the origin of the African ape and human clade. Evol. Anthropol. 21. 10–23.
- Böhme, M., Spassov, N., Fuss, J., Tröscher, A., Deane, A.S., Prieto, J., Kirscher, U., Lechner, T., Begun, D.R., 2019. A new Miocene ape and locomotion in the ancestor of great apes and humans. Nature 575, 489–493.
- Burke, A.C., Nelson, C.E., Morgan, B.A., Tabin, C., 1995. Hox genes and the evolution of vertebrate axial morphology. Development 121, 333-346.
- Cheverud, J.M., 1982. Phenotypic, genetic, and environmental morphological integration in the cranium. Evolution 36, 499–516.
- Cheverud, J.M., 1988. A comparison of genetic and phenotypic correlations. Evolution 42 958-968
- Cheverud, J.M., 1996. Developmental integration and the evolution of pleiotropy. Am, Zool, 36, 44-50.
- Conaway, M.A., Schroeder, L., von Cramon-Taubadel, N., 2018. Morphological integration of anatomical, developmental, and functional postcranial modules in the crab-eating macaque (Macaca fascicularis). Am. J. Phys. Anthropol. 166, 661-670
- de Oliveira, F.B., Porto, A., Marroig, G., 2009. Covariance structure in the skull of Catarrhini: a case of pattern stasis and magnitude evolution. J. Hum. Evol. 56, 417-430
- Fleagle, J.G., 2013. Primate Adaptation & Evolution. Academic Press, San Diego. Goswami, A., Polly, P.D., 2010. The influence of modularity on cranial morphological disparity in Carnivora and Primates (Mammalia). PLoS One 5, e9517.
- Goswami, A., Smaers, J.B., Soligo, C., Polly, P.D., 2014. The macroevolutionary consequences of phenotypic integration: from development to deep time. Phil. Trans. R Soc. B 369, 20130254.
- Gould, S.J., Lewontin, R.C., 1979. The spandrels of San Marco and the Panglossian paradigm: a critique of the adaptationist programme. Proc. R Soc. B 205, 581-598.
- Gould, S.J., Vrba, E.S., 1982. Exaptation-a missing term in the science of form. Paleobiology 8, 4-15.
- Grabowski, M.W., Jungers, W.L., 2017. Evidence of a chimpanzee-sized ancestor of humans but a gibbon-sized ancestor of apes. Nat. Commun. 8, 880.
- Grabowski, M.W., Porto, A., 2017. How many more? Sample size determination in studies of morphological integration and evolvability. Method. Ecol. Evol. 8, 592-603.
- Grabowski, M.W., Polk, J.D., Roseman, C.C., 2011. Divergent patterns of integration and reduced constraint in the human hip and the origins of bipedalism. Evolution 65, 1336-1356.
- Hallgrímsson, B., Jamniczky, H., Young, N.M., Rolian, C., Parsons, T.E., Boughner, J.C., Marcucio, R.S., 2009. Deciphering the palimpsest: studying the relationship between morphological integration and phenotypic covariation. Evol. Biol. 36, 355-376.
- Hansen, T.F., Houle, D., 2008. Measuring and comparing evolvability and constraint in multivariate characters. J. Evol. Biol. 21, 1201–1219.
- Iacobucci, D., Schneider, M.J., Popovich, D.L., Bakamitsos, G.A., 2016. Mean centering helps alleviate "micro" but not "macro" multicollinearity. Behav. Res. Methods 48, 1308-1317.
- Johnson, S.E., Shapiro, L.J., 1998. Positional behavior and vertebral morphology in atelines and cebines. Am. J. Phys. Anthropol. 105, 333-354.
- Jung, H., Conaway, M.A., von Cramon-Taubadel, N., 2020. Examination of sample size determination in integration studies based on the integration coefficient of variation (ICV). Evol. Biol. 47, 293-307.
- Jung, H., Simons, E., von Cramon-Taubadel, N., 2021. Ontogenetic changes in magnitudes of integration in the macaque skull. Am. J. Phys. Anthropol. 174, 76-88.
- Kikuchi, Y., Nakatsukasa, M., Nakano, Y., Kunimatsu, Y., Shimizu, D., Ogihara, N., Tsujikawa, H., Takano, T., Ishida, H., 2015. Morphology of the thoracolumbar spine of the middle Miocene hominoid Nacholapithecus kerioi from northern Kenya. J. Hum. Evol. 88, 25-42.
- Klingenberg, C.P., 2014. Studying morphological integration and modularity at multiple levels: concepts and analysis. Phil. Trans. R Soc. B 369, 20130249.
- Latimer, B., Ward, C.V., 1993. The thoracic and lumbar vertebrae. In: Walker, A., Leakey, R.E. (Eds.), The Nariokotome Homo erectus Skeleton. Harvard University Press, Cambridge, pp. 267–293.
- Lawler, R.R., 2008. Morphological integration and natural selection in the postcranium of wild Verreaux's sifaka (Propithecus verreauxi verreauxi). Am. J. Phys. Anthropol. 136, 204-213.
- Lewton, K.L., 2012. Evolvability of the primate pelvic girdle. Evol. Biol. 39, 126-139. Lieberman, D., 2011. The Evolution of the Human Head. Harvard University Press, Cambridge.

- Linden, A.V., Hedrick, B.P., Kamilar, J.M., Dumont, E.R., 2019. Atlas morphology, scaling and locomotor behavior in primates, rodents and relatives (Mammalia: Euarchontoglires). Zool. J. Linn. Soc. 185, 283-299.
- Machnicki, A.L., Lovejoy, C.O., Reno, P.L., 2016. Developmental identity versus typology: lucy has only four sacral segments. Am. J. Phys. Anthropol. 160, 729-739
- Manfreda, E., Mitteroecker, P., Bookstein, F.L., Schaefer, K., 2006. Functional morphology of the first cervical vertebra in humans and nonhuman primates. Anat. Rec. B 289, 184-194.
- Marroig, G., Cheverud, J.M., 2004. Cranial evolution in sakis (Pithecia, Platyrrhini) I: interspecific differentiation and allometric patterns, Am. I. Phys. Anthropol. 125. 266 - 278.
- Marroig, G., Cheverud, I.M., 2005, Size as a line of least evolutionary resistance: diet and adaptive morphological radiation in New World monkeys. Evolution 59, 1128-1142.
- Marroig, G., Shirai, L.T., Porto, A., de Oliveira, F.B., De Conto, V., 2009. The evolution of modularity in the mammalian skull II: evolutionary consequences. Evol. Biol. 36, 136-148,
- Melo, D., Garcia, G., Hubbe, A., Assis, A.P., Marroig, G., 2015. EvolQG-An R package for evolutionary quantitative genetics. F1000Research 4. https://doi.org/ 10 12688/f1000research 7082 3
- Nakatsukasa, M., 2008. Comparative study of Moroto vertebral specimens. J. Hum. Evol. 55, 581-588.
- Nakatsukasa, M., 2019. Miocene ape spinal morphology: the evolution of orthogrady. In: Been, E., Gómez-Olivencia, A., Kramer, P.A. (Eds.), Spinal Evolution: Morphology, Function, and Pathology of the Spine in Hominoid Evolution. Springer, Cham. pp. 73-96.
- Nalley, T.K., Grider-Potter, N., 2015. Functional morphology of the primate head and
- neck. Am. J. Phys. Anthropol. 156, 531–542.

 Nalley, T.K., Grider-Potter, N., 2017. Functional analyses of the primate upper cervical vertebral column. J. Hum. Evol. 107, 19–35.
- Nowicki, J.L., Burke, A.C., 2000. Hox genes and morphological identity: axial versus lateral patterning in the vertebrate mesoderm. Development 127, 4265-4275.
- Olson, E.C., Miller, R.L., 1958. Morphological Integration. University of Chicago Press, Chicago.
- Pilbeam, D.R., 1996. Genetic and morphological records of the Hominoidea and hominoid origins: a synthesis. Mol. Phylogenet. Evol. 5, 155-168.
- Pilbeam, D.R., Lieberman, D.E., 2017. Reconstructing the last common ancestor of chimpanzees and humans. In: Muller, M.N., Wrangham, R.W., Pilbeam, D.R. (Eds.), Chimpanzees and Human Evolution. Harvard University Press, Cambridge, pp. 22-141.
- Porto, A., de Oliveira, F.B., Shirai, L.T., De Conto, V., Marroig, G., 2009. The evolution of modularity in the mammalian skull I: morphological integration patterns and magnitudes. Evol. Biol. 36, 118-135.
- R Core Team, 2020. R: A Language and Environment for Statistical Computing. R Foundation for Statistical computing, Vienna, Austria. http://www.R-project.org.
- Randau, M., Goswami, A., 2017. Unravelling intravertebral integration, modularity and disparity in Felidae (Mammalia). Evol. Dev. 19, 85-95.
- Rolian, C., Lieberman, D.E., Hallgrímsson, B., 2010. The coevolution of human hands and feet. Evolution 64, 1558-1568.
- Russo, G.A., Shapiro, L.J., 2011. Morphological correlates of tail length in the catarrhine sacrum. J. Hum. Evol. 61, 223-232.
- Russo, G.A., Shapiro, L.J., 2013. Reevaluation of the lumbosacral region of Oreopithecus bambolii. J. Hum. Evol. 65, 253-265.
- Russo, G.A., Williams, S.A., 2015. "Lucy" (A.L. 288-1) had five sacral vertebrae. Am. J. Phys. Anthropol. 156, 295-303.
- Sanders, W.J., Bodenbender, B.E., 1994. Morphometric analysis of lumbar vertebra UMP 67-28: implications for spinal function and phylogeny of the Miocene Moroto hominoid. J. Hum. Evol. 26, 203-237.
- Savell, K.R., Auerbach, B.M., Roseman, C.C., 2016. Constraint, natural selection, and the evolution of human body form. Proc. Natl. Acad. Sci. USA 113, 9492-9497.
- Shapiro, L.J., 1993. Functional morphology of the vertebral column in primates. In: Gebo, D.L. (Ed.), Postcranial Adaptation in Non-human Primates. Northern Illinois University Press, DeKalb, pp. 121-149.
- Shapiro, L.J., Kemp, A.D., 2019. Functional and developmental influences on intraspecific variation in catarrhine vertebrae. Am. J. Phys. Anthropol. 168, 131–144.
- Shirai, L.T., Marroig, G., 2010. Skull modularity in neotropical marsupials and monkeys: size variation and evolutionary constraint and flexibility. J. Exp. Zool. B Mol. Dev. Evol. 314, 663-683.
- Susanna, I., Alba, D.M., Almécija, S., Moya-Sola, S., 2014. The vertebral remains of the late Miocene great ape Hispanopithecus laietanus from can Llobateres 2 (Vallès-Penedès basin, NE Iberian peninsula). J. Hum. Evol. 73, 15-34.
- Villamil, C.I., 2018. Phenotypic integration of the cervical vertebrae in the Hominoidea (Primates). Evolution 72, 490-517.
- Villmoare, B., Fish, J., Jungers, W., 2011. Selection, morphological integration, and strepsirrhine locomotor adaptations. Evol. Biol. 38, 88–99.
- von Cramon-Taubadel, N., Frazier, B.C., Lahr, M.M., 2007. The problem of assessing landmark error in geometric morphometrics: theory, methods, and modifications. Am. J. Phys. Anthropol. 134, 24-35.
- Ward, C.V., 1993. Torso morphology and locomotion in Proconsul nyanzae. Am. J. Phys. Anthropol. 92, 291-328.

- Ward, C.V., 2015. Postcranial and locomotor adaptations of hominoids. In: Henke, W., Tattersall, I. (Eds.), Handbook of Paleoanthropology, Second Edition. Springer, Berlin, pp. 1363–1386.
- Ward, C.V., Hammond, A.S., Plavcan, J.M., Begun, D.R., 2019. A late Miocene hominid partial pelvis from Hungary. J. Hum. Evol. 136, 102645.
 Wellik, D.M., 2007. *Hox* patterning of the vertebrate axial skeleton. Dev. Dynam.
- 236, 2454-2463.
- Wellik, D.M., Capecchi, M.R., 2003. Hox10 and Hox11 genes are required to globally
- pattern the mammalian skeleton. Science 301, 363–367.
 Wiley, D.F., Amenta, N., Alcantara, D.A., Ghosh, D., Kil, Y.J., Delson, E., Harcourt-Smith, W., Rohlf, F.J., Katherine, S.J., Hamann, B., 2005. Evolutionary Morphing. https://escholarship.org/uc/item/4k5991zk.
- Williams, S.A., 2010. Morphological integration and the evolution of knucklewalking, J. Hum, Evol. 58, 432-440.
- Williams, S.A., 2012. Variation in anthropoid vertebral formulae: implications for homology and homoplasy in hominoid evolution. J. Exp. Zool. 318,
- Williams, S.A., Middleton, E.R., Villamil, C.I., Shattuck, M.R., 2016. Vertebral numbers and human evolution. Am. J. Phys. Anthropol. 159, 19–36.
 Williams, S.A., Prang, T.C., Meyer, M.R., Russo, G.A., Shapiro, L.J., 2020. Reevaluating
- bipedalism in *Danuvius*. Nature 586, E1–E3.
- Young, N.M., Wagner, G.P., Hallgrímsson, B., 2010. Development and the evolvability of human limbs. Proc. Natl. Acad. Sci. USA 107, 3400–3405.